Advances in Cognitive Systems 2 (2012) 77-94 Submitted 9/2012; published 12/2012

# Seeing Unseeability to See the Unseeable

**Siddharth Narayanaswamy** SIDDHARTH@IFFSID.COM
**Andrei Barbu** ANDREI@0XAB.COM
**Jeffrey Mark Siskind** QOBI@PURDUE.EDU
School of Electrical & Computer Engineering, Purdue University, West Lafayette, IN 47907 USA

## Abstract

We present a framework that allows an observer to determine the structure of occluded portions of an assembly by estimating the structure of those occluded portions in a way that is consistent with visible image evidence and world knowledge. Doing this requires determining which portions of the assembly are occluded in the first place. Since each process relies on the other, we determine a solution to both problems in tandem. We extend our framework to determine confidence of one's assessment of which portions of an observed assembly are occluded, and the estimate of the structure of those occluded portions, by determining the sensitivity of one's assessment to potential new observations. We further extend our framework to determine a robotic action whose execution would allow a new observation that would maximally increase one's confidence. The formulation of our framework further allows for the elegant integration of evidence across modalities. We demonstrate such ability through the integration of information from natural-language statements describing the assembly that aid the estimation of its structure and the simultaneous resolution of both visual and linguistic ambiguity.

## 1. Introduction

> [T]here are known knowns; there are things we know we know. We also know there are known unknowns; that is to say we know there are some things we do not know. But there are also unknown unknowns — the ones we don't know we don't know.
>
> Donald Rumsfeld (12 February 2002)

People exhibit the uncanny ability to see the unseeable. The colloquial exhortation *You have eyes in the back of your head!* expresses the assessment that someone is making correct judgments as if they could see what is behind them, but obviously cannot. People regularly determine the properties of occluded portions of objects from observations of visible portions of those objects using general world knowledge about the consistency of object properties. Psychologists have demonstrated that the world knowledge that can influence perception can be high level, abstract, and symbolic, and not just related to low-level image properties such as object class, shape, color, motion, and texture. For example, Freyd et al. (1988) showed that physical forces, such as gravity, and whether such forces are in equilibrium, due to support and attachment relations, influences visual perception of object location in adults. Baillargeon (1986, 1987) showed that knowledge of substantiality, the fact that solid objects cannot interpenetrate, influences visual object perception in young infants.

Streri and Spelke (1988) showed that knowledge about object rigidity influences both visual and haptic perception of those objects in young infants. Moreover, such influence is cross modal: observable haptic perception influences visual perception of unobservable properties and observable visual perception influences haptic perception of unobservable properties. Wynn (1998) showed that material properties of objects, such as whether they are countable or mass substances, along with abstract properties, such as the number of countable objects and the quantity of mass substances, and how they are transferred between containers, influences visual perception in young infants. Similar results exist for many physical properties such as relative mass, momentum, etc. These results demonstrate that people can easily integrate information from multiple sources together with world knowledge to see the unseeable.

People so regularly invoke the ability to see the unseeable that we often don't realize that we do so. If you observe a person entering the front door of a house and later see them appear from behind the house without seeing them exit, you easily see the unseeable and conclude that there must be an unseen door to the house. But if one later opens a curtain covering a large living-room bay window in the front of the house so that you see through the house and see the back door you no longer need to invoke the ability to see the unseeable. A more subtle question then arises: when must you invoke the ability to see the unseeable? In other words how can you see unseeability, the inability to see? This question becomes particularly thorny since, as we will see, it can involve a chicken-and-egg problem: seeing the unseen can require seeing the unseeability of the unseen and seeing the unseeability of the unseen can require seeing the unseen.

The ability to see unseeability and to see the unseeable can further dramatically influence human behavior. We regularly and unconsciously move our heads and use our hands to open containers to render seeable what was previously unseeable. To realize that we need to do so in the first place, we must first see the unseeability of what we can't see. Then we must determine how to best use our perceptual, motor, and reasoning affordances to remedy the perceptual deficiency.

We present a general computational framework for seeing unseeability to see the unseeable. We formulate and evaluate a particular instantiation of this general framework in the context of a restricted domain, namely LINCOLN LOGS, a children's assembly toy where one constructs assemblies from a small inventory of logs. Two relevant aspects of this domain facilitate its use for investigating our general computational framework: (a) LINCOLN LOG assemblies suffer from massive occlusion and (b) a simple but rich expression of world knowledge, in the form of constraints on valid assemblies, can mitigate the effects of such occlusion. While LINCOLN LOGS are a children's toy, this domain is far from a toy when it comes to computer vision. The task of structure estimation, determining, from an image, the correct combination of component logs used to construct an assembly and how they are combined, is well beyond the state of the art. Not only is the computer-vision problem for this domain immensely difficult—occlusion, luminance variation, and a distinct paucity of features all encumber the process—the computational problem itself affords a richness and complexity that is not readily apparent.

We present methods for seeing the unseeable (in Section 2) and seeing unseeability (in Section 3) based on precise computation of the maximum-likelihood structure estimate. Section 4 presents a rational basis for determining confidence in one's structure estimate despite unseeability based on precise computation of the amount of evidence needed to override a uniform prior on the unseeable.

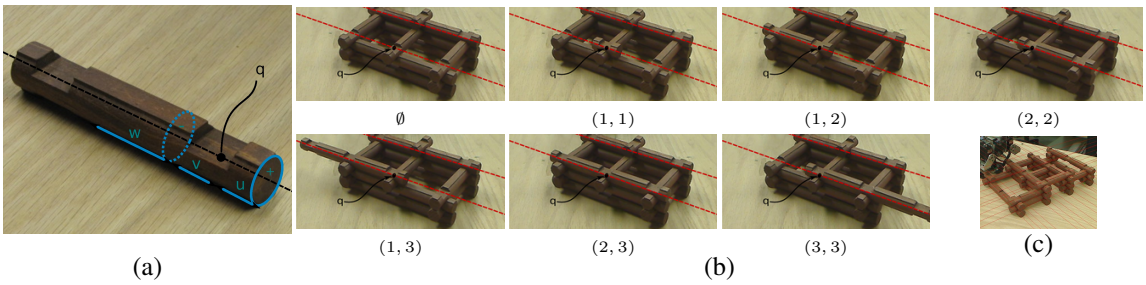


*Figure 1.* We generate two kinds of random variables for each grid position $q$: log-feature variables (a) that encode the observed image evidence for portions of logs and log-occupancy variables (b) that encode the structure. The overall process of structure estimation involves determining the unknown values of the log-occupancy variables (b) from the observed image evidence represented through provided values of the log-feature variables (a). This process is mediated through the constraints shown in Figure 2(a). (a) The Boolean log-feature variables $Z_q^+$, $Z_q^-$, $Z_q^u$, $Z_q^v$, and $Z_q^w$ encode the presence of the specified image features for grid position $q$. (b) The log-occupancy variable $Z_q$ for grid position $q$ takes one of a finite set of possible values: $\emptyset$ to denote that $q$ is unoccupied and $(m, n)$ to denote occupancy by the $m^{\text{th}}$ notch of an $n$-notch log. (c) Example of the underlying symbolic grid of a LINCOLN LOG assembly.

Section 5 presents an active-vision decision-making process for determining rational behavior in the presence of unseeability based on precise computation of which of several available perception-enhancing actions one should take to maximally improve the confidence in one's structure estimate. Such capability is bootstrapped by our framework's capacity to integrate evidence from different views, both *imagined* and *actual*. Section 6 further highlights the elegance of our framework by demonstrating the integration of evidence *across* modalities; using natural-language descriptions to aid in resolving ambiguities in structure estimation.

## 2. Structure Estimation

Speech recognizers use a human language model, on utterances in a generative linguistic domain, to improve recognition accuracy over the raw recognition rate of the phoneme detectors. Analogously, Siddharth et al. (2011) use a visual language model, on compositional visual structures in a generative visual domain, to improve recognition accuracy over the raw recognition rate of the part detectors. In this approach, a complex object is constructed out of a collection of parts taken from a small part inventory. A language model, in the form of a stochastic constraint-satisfaction problem (CSP; Lauriere, 1978), characterizes the constrained way object parts can combine to yield a whole object and significantly improves the recognition rate of the whole structure over the infinitesimally small recognition rate that would result from unconstrained application of the unreliable part detectors. Unlike the speech-recognition domain, where (except for coarticulation) there is acoustic evidence for all phonemes, in the visual domain there may be components with no image evidence due to occlusion. A novel aspect of applying a language model in the visual domain instead of the linguistic domain is that it can additionally help in recovering occluded information.

This approach is demonstrated in the domain of LINCOLN LOGS, a children's assembly toy with a small part inventory, namely, 1-, 2-, and 3-notch logs. In a grammatical LINCOLN LOG assembly, all logs lie on a symbolic grid imposed over the structure (Figure 1c). The structure of an assembly can be completely and unambiguously described by specifying the occupancy at each grid position

2-notch logs occupy 2 adjacent grid points
3-notch logs occupy 3 adjacent grid points
1- and 2-notch logs must be supported at all notches
3-notch logs must be supported in at least 2 notches
log ends must be at the ends of logs
short segments indicate occupancy above or below
long segments indicate presence of a multi-notch log

(a)

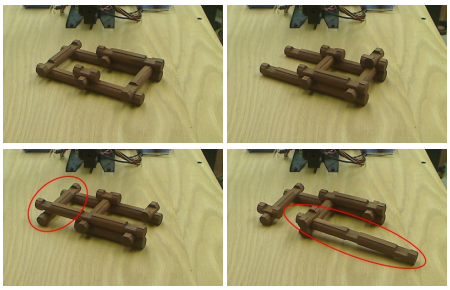

(b)

*Figure 2.* (a) The constraints that encode the grammar of LINCOLN LOGS. (b, top) Examples of structures that satisfy the grammar. (b, bottom) Examples of structures that do not satisfy the grammar, because of unsupported logs.

(Figure 1b). Not all possible occupancy descriptions denote stable, physically realizable structures. The space of valid structures can be specified by local constraints on the occupancy of adjacent grid positions, as shown in Figure 2(a). Enforcing these constraints over the entire structure renders some assemblies grammatical and others ungrammatical, as shown in Figure 2(b).

LINCOLN LOGS, being cylindrical, generate two predominant image features: *log ends*, ellipses that result from the perspective projection of circular log ends, and *log segments*, line segments that result from the perspective projection of cylindrical walls. Boolean random variables $Z^+$ and $Z^-$ are constructed to encode the presence of log-end features in the image. Similar Boolean random variables $Z^u$, $Z^v$, and $Z^w$ are constructed to encode the presence of log-segment features in the image. There is one instance of each such variable, $Z_q^+$, $Z_q^-$, $Z_q^u$, $Z_q^v$, and $Z_q^w$, for each grid position $q$, as shown in Figure 1(a). We also construct a discrete random variable $Z_q$ for each grid position $q$ that ranges over its possible occupancies in the structure, as shown in Figure 1(b). In the exposition below, we use $\mathbf{Z}^+$, $\mathbf{Z}^-$, $\mathbf{Z}^u$, $\mathbf{Z}^v$, $\mathbf{Z}^w$, and $\mathbf{Z}$ to denote the collections of the variables $Z_q^+$, $Z_q^-$, $Z_q^u$, $Z_q^v$, $Z_q^w$, and $Z_q$ for all of the grid positions $q$ in the problem at hand.

The values of the log-feature variables are determined directly from the image. The values of the log-occupancy variables, however, cannot be directly observed. The essence of structure estimation is to determine the values of the log-occupancy variables. This is done by formulating and solving a constraint satisfaction problem that mutually constraints the log-feature and log-occupancy variables, using Algorithm 1. The constraints are formalizations of the world knowledge in Figure 2(a). Because the image evidence as encoded in the log-feature variables is noisy, unreliable, and incomplete (due to occlusion), we cannot treat this as a symbolic CSP and instead treat this as a stochastic CSP. Within this stochastic framework, structure estimation is performed by establishing priors over the random variables $Z_q^+$, $Z_q^-$, $Z_q^u$, $Z_q^v$, and $Z_q^w$ that correspond to log features using image evidence and establishing a uniform prior over the random variables $Z_q$ that correspond to the latent structure. The random variables that correspond to log features are marginalized [1] and the resulting marginal

1. Marginalization is the process of deriving the joint distribution $M$ of a *subset*, say $\{A\}$, of the constituent variables of a joint distribution over all of the variables, say $\{A, B, C\}$. We compute such as $M = \Pr(A) = \sum_{B,C} \Pr(A, B, C)$. We utilize this in order to be able to derive the distribution over log occupancies, which is what we want, from the joint distribution over log occupancies and observed image evidence, which is what we have. Historically, this term evolved from the practice of displaying the values of a joint distribution $\Pr(A, B)$ as a two-

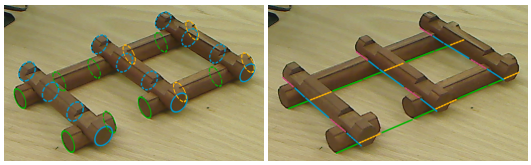

(a) (b)

| size (X×YX×YZ×Z) | # grid points | possible structures | valid structures |
|---|---|---|---|
| $2 \times 2 \times 2 \times 2$ | 8 | $5 \times 10^6$ | 233 |
| $2 \times 3 \times 2 \times 2$ | 12 | $10^{10}$ | 1341 |
| $2 \times 3 \times 3 \times 2$ | 16 | $10^{13}$ | 6667 |
| $3 \times 2 \times 2 \times 3$ | 12 | $10^{10}$ | 5461 |
| $3 \times 2 \times 2 \times 3$ | 18 | $10^{15}$ | 670179 |

(c)

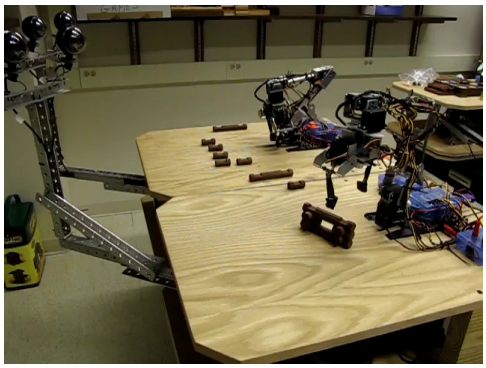

(d)

*Figure 3.* Example visibility estimates for (a) log ends and (b) log segments. Green and orange indicate the visible and occluded features for even layers, while blue and magenta indicate visible and occluded features for odd layers. (c) Size of the space of LINCOLN LOG assemblies for given grid sizes. $XZ$ is the ground plane while $YX$ and $YZ$ are the heights of the assembly along the respective ground-plane axes. (d) Our robotic environment for performing structure estimation with a rotating head to image the assembly from different viewpoints and a robot arm to disassemble the assembly.

distribution is conditioned on the language model $\Phi$ to enforce the constraints from Figure 2(a). Finally, the assignment to the collection, $\mathbf{Z}$, of random variables $Z_q$, that maximizes this conditional marginal probability is computed:

$$\underset{\mathbf{Z}}{\operatorname{argmax}} \sum_{\substack{\mathbf{Z}^+,\mathbf{Z}^-,\mathbf{Z}^u,\mathbf{Z}^v,\mathbf{Z}^w \\ \Phi[\mathbf{Z},\mathbf{Z}^+,\mathbf{Z}^-,\mathbf{Z}^u,\mathbf{Z}^v,\mathbf{Z}^w]}} \Pr\left(\mathbf{Z},\mathbf{Z}^+,\mathbf{Z}^-,\mathbf{Z}^u,\mathbf{Z}^v,\mathbf{Z}^w\right) \tag{1}$$

While this method can determine the conditional probability distribution over consistent structures given image evidence, doing so is combinatorially intractable. To see why this is so, consider a simple $2 \times 2 \times 2$ grid representing the underlying structure of a hypothetical LINCOLN LOG assembly. Even for so small an assembly, since each grid position can take one of seven possible values, the total number of possibilities ($7^8 \approx 5 \times 10^6$), exponential in the number of grid points, is huge. This is due to the generative nature of the LINCOLN LOG domain. We illustrate this point further with Figure 3(c), where we enumerate the number of possible structures and how many of such are valid given our system of constraints, for a few relatively small grid sizes.

To compute Equation 1, we employ algorithms for each of the constituent processes that help ameliorate this intractability. These algorithms prune the space so as not to enumerate all possible structures, and hence cannot obtain the distribution over structures. The conditional marginalization process is made tractable by pruning assignments to the random variables that violate the grammar $\Phi$ using arc consistency (Mackworth, 1977). The maximization process is made tractable by using a branch-and-bound algorithm (Land & Doig, 1960) that maintains upper and lower bounds on the maximal conditional marginal probability. Instead of determining the distribution over structures,

dimensional table with rows for the $A$ entries and columns for the $B$ entries. The values of $\Pr(A)$ were derived by summing along the columns to yield a new row at the bottom *margin* of the table. The values of $\Pr(B)$ were derived by summing along the rows to yield a new column at the right *margin* of the table. This led to $\Pr(A)$ and $\Pr(B)$ being referred to as *marginal* probabilities and the derivation process as *marginalization*.

*Algorithm 1.* The structure-estimation algorithm as described in Section 2.

```
grid-positions ← (∀grid-position∈grid) uniform({∅, (1,1), (1,2), (2,2), (1,3), (2,3), (3,3)});
log-features ← (∀log-feature∈grid) detector(log-feature,image);
best-probability ← −∞;
while csp-solutions-exist() do
    probability ← ∏_{bound(log-features)} Pr(log-feature) ∏_{bound(grid-positions)} Pr(grid-position);
    if (∀log-features)bound(log-feature) ∧ (∀grid-positions)bound(grid-position) then
        if probability > best-probability then
            best-probability ← probability;
            best-structure ← grid-positions;
        end
        backtrack();
    end
    if probability < best-probability then backtrack();
    bind(select(unbound(grid-position ∪ log-feature)));
    arc-consistency(constraints);
    if inconsistent() then backtrack()
end
```

this yields a single most-likely consistent structure given the image evidence, along with its probability. Algorithm 1 gives pseudo-code for the structure-estimation process.

## 3. Visibility Estimation

Image evidence for the presence or absence of each log feature is obtained independently. Each log feature corresponds to a unique local image property when projected to the image plane under the known camera-relative pose. A prior over the random variable associated with a specific log feature can be determined with a detector that is focused on the expected location and shape of that feature in the image given the projection. This assumes that the specific log feature is visible in the image, and not occluded by portions of the assembly between the camera and that log feature. We show example visibility of log-end and log-segment features for a simple LINCOLN LOG assembly in Figure 3(a,b). When the log feature $f$, a member of the set $\{+, -, u, v, w\}$ of the five feature classes defined above, at a position $q$, is not visible, the prior can be taken as uniform, allowing the grammar to fill in unknown information. We represent the visibility of a feature $f$ at position $q$ by the boolean variable $V_q^f$, where:

$$\Pr(Z_q^f = \mathbf{true}) \propto \text{image evidence} \qquad \text{when } V_q^f = \mathbf{true} \tag{2a}$$

$$\Pr(Z_q^f = \mathbf{false}) = \frac{1}{2} \qquad \text{otherwise.} \tag{2b}$$

In order to do so, it is necessary to know which log features are visible and which are occluded so that image evidence is only applied to construct a prior on visible log features, using Equation 2(a), and a uniform prior is constructed for occluded log features, using Equation 2(b). Thus, in Rumsfeld's terminology, one needs to know the known unknowns in order to determine the unknowns. This creates a chicken-and-egg problem. To determine whether a particular log feature is visible, one must know the composition of the structure between that feature and the camera. Likewise, to

determine the structure composition, one must know which log features are visible. While earlier work (Siddharth, Barbu, & Siskind, 2011) demonstrated successful automatic determination of log occupancy at occluded log positions, it could only do so given manual annotation of log-feature visibility. In other words, while $Z_q$ was automatically inferred, it required manual annotation of $V_q^f$. Further, manual annotation of $V_q^f$ required implicit human awareness of $Z_q$.

We extend this prior work to automatically determine visibility of log features in tandem with log occupancy. Our novel contribution in this section is mutual automatic determination of both $Z_q$ and $V_q^f$ solving the chicken-and-egg problem inherent in doing so with an iterative algorithm reminiscent of expectation maximization (Dempster, Laird, & Rubin, 1977). We start with an initial estimate of the visibility of each log feature. We apply the structure-estimation procedure to estimate the occupancy of each symbolic grid position and use the estimated structure to recompute a new estimate of log-feature visibility and iterate this process until a fixpoint is reached. There are two crucial components in this process: determining the initial log-feature visibility estimate and reestimating log-feature visibility from an estimate of structure.

We determine the initial log-feature visibility estimate, $V_q^f$, by assuming that the structure is a rectangular prism whose top face and two camera-facing front faces are completely visible, and whose other faces are not. No assumptions are made about the constituents of the structure, its pose, or the camera views used. We use the camera-relative pose of the symbolic grid (which can be determined without any knowledge of the structure) together with the maximal extent of each of the three symbolic grid axes, three small integers which are currently specified manually, to determine the visible faces. We determine the image positions for four corners of the base of this rectangular prism and the bottommost three such image positions as they correspond to the endpoints of the lower edges of the two frontal faces. It is possible that one of these faces is nearly parallel to the camera axis and thus invisible. We determine that this is the case when the angle subtended by the two lower edges is less than $110^\circ$ and discard the face whose lower edge has minimal image width. This process does nothing more than establish that, in the absence of a structure estimate from which to derive visibility, the front and top faces of the grid are the only parts for which the log-feature random variables have image evidence as their support, using Equation 2(a). All other parts of the grid are taken to have the uniform distribution as their support, using Equation 2(b), as a means of saying that we assume nothing about them.

We update the log-feature visibility estimate from a structure estimate by rendering the structure in the context of the known camera-relative pose of the symbolic grid. We characterize each log feature with a fixed number of points, equally spaced around circular log ends or along linear log segments and trace a ray from each such point's 3D position to the camera center, asking whether that ray intersects some bounding cylinder for a log in the estimated structure. We take a log feature to be occluded when 60% or more of such rays intersect logs in the estimated structure. Structure estimation isn't adversely affected by a moderate number of log features incorrectly labeled as occluded because it can use the grammar to determine occupancy of the corresponding grid positions.

We perform such rendering efficiently by rasterization. We begin with an empty bitmap, iterate over each log feature and each occupied grid position that lies between that log feature and the camera center, and render a projection of the bounding cylinder of the log at that grid position on the bitmap.

*Algorithm 2.* The visibility-estimation algorithm as described in Section 3, using Algorithm 1.

visible ← *top and front of structure*;
current-structure ← ∅;
**repeat**
  previous-structure ← current-structure;
  current-structure ← `structure-estimation` $((\forall_{\text{log-feature} \notin \text{visible}}) \Pr(\text{log-feature}) = \frac{1}{2})$;
  visible ← ∅;
  rendered-image ← `render-structure` (current-structure);
  **forall the** log-features ∈ grid **do**
    **if** `is-visible` (log-feature, rendered-image) **then** visible ← visible ∪ {log-feature}
  **end**
**until** previous-structure = current-structure;

This renders all possible occluders for each log feature, allowing one to determine visibility by counting the rendered pixels at points that correspond to the projected rays.

The above process might not reach a fixpoint and instead enter an infinite loop of pairs of visibility and structure estimates. In practice, this process reaches a fixpoint or enters a short loop within three to four iterations, making loop detection straightforward. When a loop is detected, we select the structure in the loop with the highest probability estimate. Algorithm 2 provides the pseudo-code that summarizes the above process.

## 4. Structure-Estimation Confidence

While the structure-estimation process can determine the occupancy of a small number of grid positions when only a single set of occupancy values is consistent with the grammar and the image evidence, it is not clairvoyant; it cannot determine the structure of an assembly when a large part of that assembly is occluded and many different possible structures are consistent with the image evidence. In this case, we again have an issue of unknowns vs. known unknowns: how can one determine one's confidence in one's structure estimation? If we could determine the conditional distribution over consistent structures given image evidence, $\Pr(\mathbf{Z}|I)$, a measure of confidence could be entropy of this distribution, $H(\mathbf{Z}|I)$. However, as discussed previously, computing this distribution is intractable and consequently so is computing its entropy.[2] Thus we adopt an alternate means of measuring confidence in the result of the structure-estimation process.

Given a visibility estimate, $V_q^f$, structure estimate, $\mathbf{Z}$, and priors on random variables associated with log features computed with image evidence, $Z_q^f$, one can marginalize over the random variables associated with visible log features and compute the maximum-likelihood assignment to the random variables associated with occluded log features, $\hat{\mathbf{Z}}^f$, consistent with a given structure estimate:

$$\hat{\mathbf{Z}}^f = \underset{\substack{Z_q^f \\ V_q^f = \textbf{false}}}{\operatorname{argmax}} \sum_{\substack{Z_q^f \\ V_q^f = \textbf{true}}} \Pr(\mathbf{Z}, \mathbf{Z}^+, \mathbf{Z}^-, \mathbf{Z}^u, \mathbf{Z}^v, \mathbf{Z}^w)$$
$$\Phi[\mathbf{Z}, \mathbf{Z}^+, \mathbf{Z}^-, \mathbf{Z}^u, \mathbf{Z}^v, \mathbf{Z}^w]$$

2. The entropy $H(Z)$ of a random variable $Z$ is $\sum_{z \in Z} \Pr(z) \log \Pr(z)$. It measures the information content of a random variable, or lack thereof. Computing this requires summing over all elements in $Z$.

One can then ask the following question: what is the maximal amount $\delta$ that one can shift the probability mass on the occluded log-feature random variables *away* from the uniform prior, reassigning it to the opposite element of its support, such that estimated structure remains the same? Or in simpler terms: *Assume an initial structure estimate derived from a uniform prior over occluded log features. How much hypothetical evidence for such features is needed to change my mind about the structure?* We compute $\delta$ using a modified structure-estimation step:

$$\operatorname*{argmax}_{\substack{\mathbf{Z} \\ \Phi[\mathbf{Z},\mathbf{Z}^+,\mathbf{Z}^-,\mathbf{Z}^u,\mathbf{Z}^v,\mathbf{Z}^w]}} \sum_{\mathbf{Z}^+,\mathbf{Z}^-,\mathbf{Z}^u,\mathbf{Z}^v,\mathbf{Z}^w} \Pr(\mathbf{Z},\mathbf{Z}^+,\mathbf{Z}^-,\mathbf{Z}^u,\mathbf{Z}^v\,\mathbf{Z}^w) = \mathbf{Z}$$

when, for all $q^f$ where $V_q^f = \textbf{false}$, $\Pr(Z_q^f = \neg\hat{Z}_q^f) = \frac{1}{2} + \delta$ and $\Pr(Z_q^f = \hat{Z}_q^f) = \frac{1}{2} - \delta$. We call such a $\delta$ the *estimation tolerance*. Then, for any estimated structure, one can make a confidence judgment by comparing the estimation tolerance to an overall tolerance threshold $\delta^*$. One wishes to select a value for $\delta^*$ that appropriately trades off false positives and false negatives in such confidence judgments: we want to minimize the cases that result in a positive confidence assessment for an incorrect structure estimate and also minimize the cases that result in a negative confidence assessment for a correct structure estimate. Because the methods we present in the next section can gather additional evidence in light of negative confidence assessment in structure estimation, the former are more hazardous than the latter because they preclude gathering additional evidence and lead to an incorrect structure estimate while the latter simply incur the cost of additional evidence gathering. Because of this asymmetry, our method is largely insensitive to the particular value of $\delta^*$ so long as it is sufficiently high to not yield excessive false positives.

One can determine the estimation tolerance by binary search for the smallest value of $\delta \in (0, 0.5)$ that results in a different estimated structure, a time-consuming process. But we don't actually need the value of $\delta$; we only need to determine whether $\delta < \delta^*$. We do this by simply asking whether the estimated structure, $\mathbf{Z}$, changes when the probabilities are shifted by $\delta^*$, i.e., $\Pr(Z_q^f = \neg\hat{Z}_q^f) = \frac{1}{2} + \delta^*$ and $\Pr(Z_q^f = \hat{Z}_q^f) = \frac{1}{2} - \delta^*$. This involves only a single new structure estimation. Initializing the branch-and-bound structure-estimation algorithm with the probability of the original structure estimate given the modified distributions for the random variables associated with occluded log features speeds this process up.

## 5. Gathering Additional Evidence

Structure estimation can be made more reliable by integrating multiple sources of image evidence. We perform structure estimation in a robotic environment, illustrated in Figure 3(d), that facilities automatically gathering multiple sources of image evidence as needed. This workspace is imaged by a camera mounted on a pendulum arm that can rotate 180° about the workspace, under computer control, to image the assembly from different viewpoints. This can be used to view portions of the assembly that would otherwise be occluded. Moreover, a robotic arm can disassemble a structure on the workspace to reveal the lower layers of a structure that would otherwise be occluded by higher layers. These methods can further be combined. Generally speaking, we seek a method for constraining a single estimate of an initial structure with multiple log features derived from different viewpoints and different stages of disassembly.

We can do this as follows. Let $\mathbf{Z}$ be a collection of random variables $Z_q$ associated with log occupancy for a given initial structure. Given multiple views $i = 1, \ldots, n$ with collections $\mathbf{Z}_i$ of random variables $Z_q^+$, $Z_q^-$, $Z_q^u$, $Z_q^v$, and $Z_q^w$ associated with the image evidence for log features from those views, we can compute:

$$\operatorname*{argmax}_{\mathbf{Z}} \sum_{\substack{\mathbf{Z}_1 \ldots \mathbf{Z}_n \\ \Phi[\mathbf{Z},\mathbf{Z}_1] \wedge \cdots \wedge \Phi[\mathbf{Z},\mathbf{Z}_n]}} \Pr\left(\mathbf{Z}, \mathbf{Z}_1, \ldots, \mathbf{Z}_n\right)$$

Two issues arise in doing this. First, though one can estimate the camera-relative pose of the structure independently for each view, this does not yield the registration between these views. There are only four possible symbolic orientations of the structure in each view so for $n$ views we need only consider $4^{n-1}$ possible combinations. We can greedily search for the combination that yields the maximum-likelihood structure estimate by incrementally adding views to the structure-estimation process and registering each added view by searching for the best among the four possible registrations. Second, in the case of partial disassembly, we need to handle the fact that the partially disassembled structure is a proper subset of the initial structure. We do this by omitting random variables associated with log features for logs that are known to have been removed in the disassembly process and not instantiating constraints that mention such omitted random variables.

We can combine the techniques from Section 4 with these techniques to yield an active-vision (Bajcsy, 1988) approach to producing a confident and correct structure estimate. One can perform structure estimation on an initial image and assess one's confidence in that estimate. If one is not confident, one can plan a new observation, entailing either a new viewpoint, a partial-disassembly operation, or a combination of the two and repeat this process until one is sufficiently confident in the estimated structure. We plan new observations by asking the following question: which of the available actions maximally increases confidence? Like before, if we could determine the conditional distribution over consistent structures given image evidence, we could select the action which maximally decreases entropy. But again, neither computing this distribution nor consequently computing its entropy is tractable, as discussed previously. Thus we adopt an alternate means of measuring increase in confidence.

Consider view $i$ of the $n$ current views. For such $i$, consider the given visibility estimates $V_{iq}^f$, priors $Z_{iq}^f$ on the log-feature random variables computed with image evidence, and a structure estimate $\mathbf{Z}$ constructed from such views. We can marginalize over random variables associated with visible log features $V_{iq}^f = \mathbf{true}$ and compute the maximum-likelihood assignment $\hat{\mathbf{Z}}^f$ to the random variables associated with occluded log features that is consistent with a given structure estimate:

$$\hat{\mathbf{Z}}^f = \operatorname*{argmax}_{Z_{iq}^f, V_{iq}^f = \mathbf{false}} \sum_{\substack{Z_{iq}^f, V_{iq}^f = \mathbf{true} \\ \Phi[\mathbf{Z},\mathbf{Z}_1] \wedge \cdots \wedge \Phi[\mathbf{Z},\mathbf{Z}_n]}} \Pr(\mathbf{Z}, \mathbf{Z}_1, \ldots, \mathbf{Z}_n)$$

We determine those log features that are invisible in all current views but visible in a new view resulting from a hypothetical action. One can then ask the following question: what is the maximal amount $\delta'$ that one can shift the probability mass on these random variables *away* from the uniform prior, reassigning it to the opposite element of its support, such that the estimated structure with the new view remains the same. In simpler terms: *Assume an initial structure estimate derived from a uniform prior over occluded log features. Imagine a hypothetical action which renders such*

*occluded log features visible. For such an imagined view, how much hypothetical evidence for such log features, in all current views, is needed to change my mind about the structure?*

For an action yielding a new view, $j$, we compute $\delta'$ as

$$\underset{\mathbf{Z}}{\operatorname{argmax}} \sum_{\substack{\mathbf{Z}_1 \ldots \mathbf{Z}_n \ \mathbf{Z}_j \\ \Phi[\mathbf{Z},\mathbf{Z}_1] \wedge \cdots \wedge \Phi[\mathbf{Z},\mathbf{Z}_n] \wedge \Phi[\mathbf{Z},\mathbf{Z}_j]}} \Pr(\mathbf{Z}, \mathbf{Z}_1, \ldots, \mathbf{Z}_n, \mathbf{Z}_j) = \mathbf{Z}$$

when $\Pr(Z_{iq}^f = \neg \hat{Z}_{iq}^f) = \frac{1}{2} + \delta$ and $\Pr(Z_{iq}^f = \hat{Z}_{iq}^f) = \frac{1}{2} - \delta \; \forall q^f : V_{jq}^f = \mathbf{true} \wedge (\forall i) V_{iq}^f = \mathbf{false}$. We perform binary search to find $\delta'$ for each hypothetical action and select the one with the lowest $\delta'$. This nominally requires sufficiently deep binary search to compute $\delta'$ to arbitrary precision. One can make this process faster by performing binary search on all hypothetical actions simultaneously and terminating when there is only one action lower than the branch point. This requires that binary search be only sufficiently deep to discriminate between the available actions.

## 6. Natural Language

An interesting feature of our framework is that it allows for elegant inclusion of information from other modalities. Natural language, for example, can be integrated into our approach to draw additional evidence for structure estimation from utterances describing the structure in question. A sentence, or set of sentences, describing a structure need not specify the structure unambiguously. Much like additional images from novel viewpoints can provide supplementary but partial evidence for structure estimation, sentences providing incomplete descriptions of structural features also can provide supplementary but partial evidence for structure estimation.

We have investigated this possibility via a small domain-specific language for describing some common features present in assembly toys. This language has: three nouns (*wall*, *window*, and *door*), four spatial relations (*left of*, *right of*, *perpendicular to*, and *coplanar to*), and one conjunction (*and*). Sentences constructed from these words can easily be parsed into logical formulas.

Analogous to how a CSP encodes the validity of an assembly through a set of constraints, such logical formulas derived from sentential descriptions can also constrain the structures to be considered. The words in our vocabulary impose five constraints:

1. A *wall* is composed of a rectangular vertical coplanar set of grid points. All grid points in the wall must be occupied.
2. A *door* is composed of a rectangular vertical coplanar set of grid points. All grid points inside the door must be unoccupied. All grid points on the door posts must be log ends facing away from the door. All grid points on the mantel must be occupied by the same log. The threshold must be unoccupied and at the bottom of the structure.
3. A *window* is similar to a door whose threshold is occupied by the same log and is not constrained to be at the bottom of the structure.
4. *Perpendicular to* constrains the grid points of two entities to lie on perpendicular axes. *Coplanar to* is analogous.
5. *Right of* or *left of* constrain the relative coordinates of the grid points of two entities.

We have given formal semantic definitions for 8 words in terms of CSP fragments. These are defined informally in English above. We omit the formal definitions since they are tedious. Nonetheless, our

implementation parses sentences containing these words and applies the rules of compositional semantics to derive an overall CSP that reflects the semantics of the sentence, from the CSP fragments that reflect the semantics of the individual words. This CSP which encodes constraints derived from natural language is then combined with the CSPs which encode constraints derived from the visual language model to perform structure estimation. We thus compute a joint multiple-view and natural-language structure estimate as follows. Let $\mathbf{Z}$ be a collection of random variables $Z_q$ associated with log occupancy for a given initial structure. Given the set of constraints $\Psi$ derived from natural language and multiple views $i = 1, \ldots, n$ with collections $\mathbf{Z}_i$ of random variables $Z_q^+$, $Z_q^-$, $Z_q^u$, $Z_q^v$, and $Z_q^w$ associated with the image evidence for log features from those views, we compute

$$\underset{\mathbf{Z}}{\operatorname{argmax}} \sum_{\substack{\mathbf{Z}_1 \ldots \mathbf{Z}_n \\ \Phi[\mathbf{Z},\mathbf{Z}_1] \wedge \cdots \wedge \Phi[\mathbf{Z},\mathbf{Z}_n] \wedge \Psi[\mathbf{Z}]}} \Pr\left(\mathbf{Z}, \mathbf{Z}_1, \ldots, \mathbf{Z}_n\right)$$

An example of how such an extension improves results is shown in Figure 6. The key idea here is that the CSP is a modality-neutral internal mental representation that can be fed information derived by vision, language, or both, allowing cross-modal inference.

A system that can accept and use such cross-modal information is in keeping with our broader research effort to model human cognition. All information that is available to the human brain is provided by means of sensory input—eyes, ears, touch, etc. To this effect, we fashion our systems to accept inputs with the same modalities as humans; i.e., raw camera input for vision, natural-language text or speech for language, and motor-control primitives for proprioception.

## 7. Results

We gathered a corpus of five different images of each of 32 different structures, each from a different viewpoint, for a total of 160 images. The structures were carefully designed so that proper subset relations exist among various pairs of the 32 distinct structures.

We first evaluated automatic visibility estimation. We performed combined visibility and structure estimation on 105 of the 160 images and compared the maximum-likelihood structure estimate to that produced by Siddharth et al. (2011) using manual annotation of visibility. For each image, we compare the maximum-likelihood structure estimate to ground truth and compute the number of errors. We do this as follows. Each one-, two-, or three-notch log in either the ground truth or estimated structure that is replaced with a different, possibly empty, collection of logs in the alternate structure counts as a single error (which may be a deletion, addition, or substitution). Further, each collection of $r$ adjacent logs with the same medial axis in the ground truth that is replaced with a different collection of $s$ logs in the estimated structure counts as $\min(r, s)$ errors. We then compute an error histogram of the number of images with fewer than $t$ errors. Figure 4(a) shows the error histograms for manual visibility annotation and automatic visibility estimation. Note that the latter performs as well as the former—our automatic visibility-estimation process appears to be reliable.

We then evaluated structure-estimation confidence assessment. We computed the false-positive rate and false-negative rate of our confidence-assessment procedure over the entire corpus of 105 images, where a false positive occurs with a positive confidence assessment for an incorrect structure estimate and a false negative occurs with negative confidence assessment for a correct structure estimate. This resulted in only three false positives and seven false negatives on our corpus.

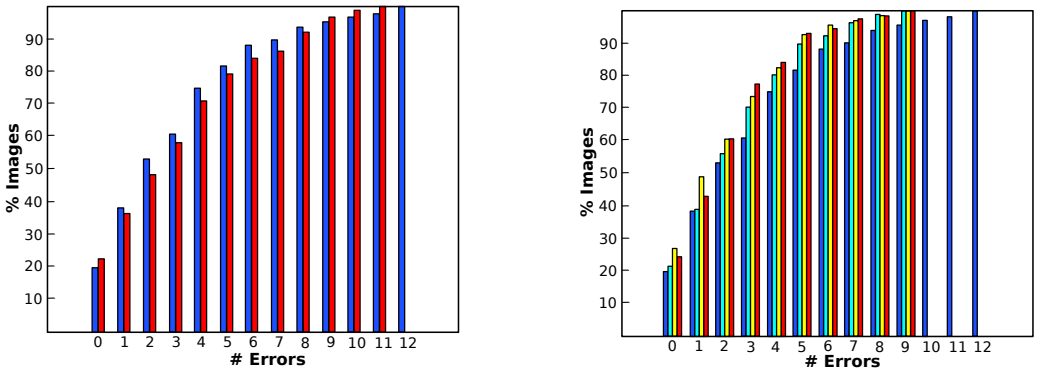


(a) (b)

*Figure 4.* (a) Error histograms for structure estimation with manual visibility annotation (in blue) and automatic visibility estimation (in red). All of the structures estimated had 12 or fewer errors. Note that the latter performs as well as the former. (b) Error histograms for the baseline structure estimation (in dark blue) and each of the active-vision process (partial disassembly in light blue, multiple views in yellow, and the combination of these in red). Note that our active-vision processes consistently reduce estimation error.

Next, we evaluated the active-vision process for performing requisite actions to improve structure estimation confidence on 90 images from our corpus. So as not to render this evaluation dependent on the mechanical reliability of our robot (which is tangential to the current paper) and focus the evaluation on the computational method, we use the fact that our corpus contains multiple views of each structure from different viewpoints to simulate moving the robot head to gather new views and the fact our corpus contains pairs of structures in a proper-subset relation to simulate using the robot to perform partial disassembly. We first evaluated simulated robot-head motion to gather new views. For each image, we took the other images of the same structure from different viewpoints as potential actions and perform our active-vision process. We next evaluated simulated robotic disassembly. For each image, we took images of proper-subset structures taken from the same viewpoint as potential actions and perform our active-vision process. We finally evaluated simulated combined robot-head motion and robotic disassembly. For each image, we took all images of proper-subset structures taken from any viewpoint as potential actions and perform our active-vision process. For each of these, we computed the error histogram at the termination of the active-vision process.

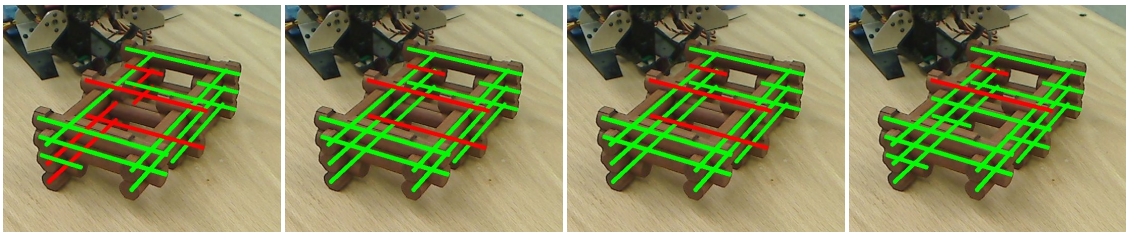

(a) (b) (c) (d)

*Figure 5.* Estimated structure through the following four methods: (a) Baseline structure estimation. (b) Partial disassembly. (c) Multiple views. (d) Combined partial disassembly and multiple views. Overlayed log color indicates correct (green) or incorrect (red) estimation of log occupancies.

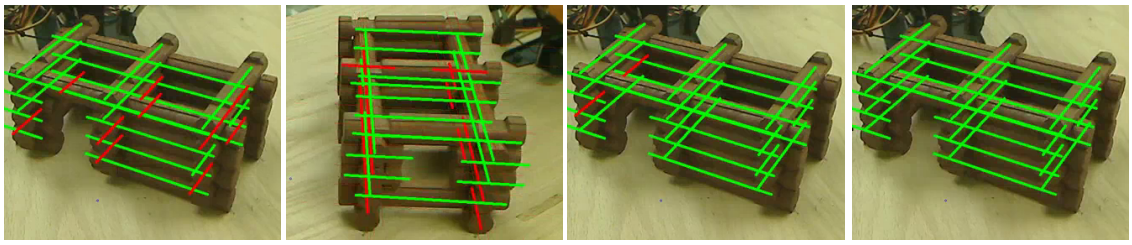

(a) View 1 (b) View 2 (c) View 1 + 2 (d) View 1 + ***Language***

*Figure 6.* An example of joint structure estimation from image evidence and natural language. (a) Structure estimation from an initial view. (b) Structure estimation from a second view alone. (c) Structure estimation using information from both views from the viewpoint of the first view. (d) Structure estimation integrating image evidence from the first view with the sentence ***window left of and perpendicular to door***. Overlayed log color indicates correct (green) or incorrect (red) estimation of log occupancies.

Figure 4(b) shows the error histograms for each of the active-vision processes together with the error histogram for baseline structure estimation from a single view on this subset of 90 images. Figure 5 shows the final estimated structure when performing each of the four processes from Figure 4(b) on the same initial image. Note that our active-vision processes consistently reduce estimation error.

We demonstrate natural-language integration in Figure 6. In (a), structure estimation is performed on a single view, which due to occlusion, is unable to determine the correct structure. A second view is acquired. Note that this second view suffers from far more occlusion than the first view and produces a far worse structure estimate (b). The information available in these two views is integrated and jointly produces a better structure estimate than either view by itself (c). However, this estimate is still imperfect. To demonstrate the utility and power of integrating visual and linguistic information, we intentionally discard the second view and construct an estimate from just a single image, together with a single linguistic description, each of which is ambiguous taken in isolation. The user provides the sentence *window left of and perpendicular to door*. Note that this sentence does not fully describe the assembly. It does not specify the number of windows and doors, their absolute positions, or the contents of the rest of the structure. Yet this sentence, together with the single image from the first view, is sufficient to correctly estimate the structure (d).

## 8. Related Work

Our work shares three overall objectives with prior work: estimating 3D structure from 2D images, determining when there is occlusion, and active vision. However, our work explores each of these issues from a novel perspective.

Prior work on structure estimation (e.g., Saxena, Sun, & Ng, 2007; Lee, Hebert, & Kanade, 2009; Gupta, Efros, & Hebert, 2010) focuses on *surface estimation*, recovering 3D surface from 2D images. In contrast, our work focuses on recovering the *constituent structure* of an assembly: what parts are used to make the assembly and how such parts are combined. Existing state-of-the-art surface reconstruction methods (e.g., Make3D, Saxena, Sun, & Ng, 2008 ) are unable to determine surface structure of the kinds of LINCOLN LOG assemblies considered here. Even if such surface estimates were successful, they are insufficient to determine the constituent structure.

Prior work on occlusion determination (e.g., Gupta, Efros, & Hebert, 2010; Hoiem, Efros, & Hebert, 2011) focuses on finding occlusion boundaries; the 2D image boundaries of occluded re-

gions, and estimating occlusion of object surfaces (e.g., Bohg et al., 2011; Mösenlechner & Beetz, 2011) in 3D using shape priors and symmetries. In contrast, our work focuses on determining occluded *parts* in the constituent structure. We see no easy way to determine occluded parts either from occlusion boundaries or from occluded surfaces since such alone are insufficient to determine even the number of occluded parts, let alone their types and positions in a 3D structure.

Prior work on active vision (e.g., Maver & Bajcsy, 1993) focuses on integrating multiple views into surface estimation and selecting new viewpoints to facilitate such in the presence of occlusion. In contrast, our work focuses on determining the confidence of constituent structure estimates and choosing an action with maximal anticipated increase in confidence. We consider not only view changes but also robotic disassembly to view object interiors. Also note that the confidence estimates used in our approach are mediated by the visual language model. We might not need to perform active vision to observe all occluded structure as it might be possible to infer part of the occluded structure. Prior work selects a new view to render occluded structure visible. We instead select an action to maximally increase confidence. Such an action might actually not attempt to view an occluded portion of the structure but rather increase confidence in a visible portion of the structure in a way that when mediated by the language model ultimately yields a maximal increase in the confidence assessment of a portion that remains occluded even with the action taken.

## 9. Conclusion

We have presented a general framework for (a) seeing the unseeable, (b) seeing unseeability, (c) a rational basis for determining confidence in what one sees, (d) an active-vision decision-making process for determining rational behavior in the presence of unseeability, and (e) the capability to integrate natural-language descriptions into the estimation process as evidence of capability to integrate information across modalities. We instantiated and evaluated our general framework in the LINCOLN LOG domain and found it to be effective. This framework has many potential extensions.

One can construct random variables to represent uncertain evidence in other modalities, such as language and speech, and augment the stochastic CSP to mutually constraint these variables together with the current random variables that represent image evidence and latent structure so that a latent utterance describes a latent structure. One can then use the same maximum-likelihood estimation techniques to produce the maximum-likelihood utterance consistent with a structure, marginalizing over image evidence. This constitutes producing an utterance that describes a visual observation.

In a similar vein, one can use the same maximum-likelihood estimation techniques to produce the maximum-likelihood sequence of robotic actions consistent with building a structure, marginalizing over utterance or image evidence. This would constitute building a structure by understanding a linguistic description of that structure or by copying a visually observed assembly.

Alternately, one can combine evidence from an uncertain visual perception of a structure with evidence from an uncertain linguistic description of that structure to reduce structure-estimation uncertainty. This would constitute using vision and language to mutually disambiguate each other. Further, one could augment one's collection of potential actions to include speech acts as well as robotic-manipulation actions and search for the action that best improves confidence. This would constitute choosing between asking someone to provide you information and seeking that informa-

tion yourself. One could determine what another agent sees from what that agent says and decide what to say so that another agent can see what is unseeable to that agent yet is seeable to you.

Overall, this can lead to a rational basis for cooperative agent behavior and a theory of the perception-cognition-action loop which incorporates mutual belief, goals, and desires where agents seek to assist each other by seeing what their peers cannot, describing such sight, and inferring what their peers can and cannot see. We are currently beginning to investigate potential extensions to our general approach and hope to present them in the future.

The ultimate goal of cognitive-systems research is to emulate human-level intelligence in an artificial agent. Humans interact physically with the real world, as perceived, and we expect our cognitive systems to do so as well. However, the real world is highly complex, metric, and noisy. Even the simple world of LINCOLN LOGS has a huge number of distinct propositions $Z_q$, $Z_q^+$, $Z_q^-$, $Z_q^u$, $Z_q^v$, and $Z_q^w$ that combine to yield an astronomical number of possible worlds as illustrated in Figure 3(c). The relationships between these propositions are governed by a metric physical process, namely projection of the 3D world onto the 2D image plane, not a logical one. Moreover, even the best current state-of-the-art computer-vision systems cannot reliably determine categorical presence of even simple image features like lines and ellipses as are needed in our task. The current mind set in the computer-vision community is that it is likely impossible to do so without high-level top-down inference. In this paper, we demonstrate several such sources of high-level top-down inference: the world knowledge encoded in the grammar, the ability to reason about visibility through imagination (the rasterized rendering process), the ability to determine confidence through counterfactual reasoning (would I change my mind if I observed something different), the ability to plan a course of action to achieve a desired knowledge-state goal, and the ability to integrate information from both language and vision. These are all forms of high-level top-down inference that outstrip those that are considered or even appreciated by the computer-vision community but are well within the province of cognitive systems. The take-home message is that computer-vision and cognitive-systems research can mutually benefit tremendously from cross-fertilization.

But in order for this to happen, it is necessary for the cognitive-systems community to understand and appreciate the richness and difficulty of computer vision. The cognitive-systems community has long developed methods for meta-reasoning: reasoning about beliefs, desires, and intentions (Moore, 1982; Bratman, Israel, & Pollack, 1988; Bratman, 1990; Cohen & Levesque, 1990; Rao & Georgeff, 1991; Hobbs et al., 1993). However, such has been formulated around symbolic representations of a small number of large-scale phenomena: ¬`CAN(SEE(DOOR))`, `IS(WALL,BETWEEN(SELF,DOOR))`, `WANT(CAN(SEE(DOOR)))`, and `DISASSEMBLE(WALL)` → ¬`IS(WALL,BETWEEN(SELF,DOOR))`. Moreover, actions are abstracted into coarse-grained symbolic representations like `DISASSEMBLE(WALL)` that do not expose the myriad low-level state changes that these objects go through as a result of such an action and how such state changes impact high-level concepts like `IS(WALL,BETWEEN(SELF,DOOR))`.

Computer vision, however, deals with a huge number of small-scale phenomena: presence or absence of the myriad pixels and edge fragments that combine to yield parts, the myriad parts that combine through articulation and deformation to yield objects, and the myriad motions and state changes that these objects go through when performing even a simple action like `DISASSEMBLE(WALL)`. Moreover, these phenomena are inherently metric: position, shape, and intensity of edge fragments, continuous parameters of articulation and deformation, and descriptions of motion in terms of ve-

locity and acceleration. Yet even at this small scale, reasoning about beliefs, desires, and intentions is beneficial. Our variables $Z_q$, $Z_q^+$, $Z_q^-$, $Z_q^u$, $Z_q^v$, and $Z_q^w$ are propositions about the state of the world. Our variables $V_q^f$ are meta-level propositions about knowledge states. One difference between our work and classical work about knowledge states is that we have many such: several for each of the many possible components and component positions. Another difference is that the relation between the two is too rich and complex to be described by a logical theory; instead we have a metric imagination process built out of a rasterizing 3D rendering engine. Another is that all these myriad variables have distinct levels of uncertainty that is metrically correlated with the low-level projection process: greater level of occlusion leads to higher-degree of uncertainty. Solving the cognitive-systems issues in a computer-vision context requires reasoning about a huge number of uncertain small-scale metric phenomena that are related by metric physical principles.

The way forward requires a bridge between the cognitive-systems and computer-vision communities. Cognitive systems will only ever be able to deal with real-world perceptual input if it accepts the fact that the propositional structure must be fine-grained (about numerous small perceptual entities that comprise any cognitive concept), metric (about actual sizes, shapes, positions, velocities, accelerations, forces, etc.), and noisy. Computer-vision systems will only ever be able to yield reliable aggregate assessments of the environment at large with high-level top-down world knowledge and inference. These two must speak a common language. We have taken a small step in demonstrating what such a language would look like in this paper.

## Acknowledgements

This work was supported, in part, by NSF Grant No. CCF-0438806, NRL Contract No. N00173-10-1-G023, ARL Cooperative Agreement No. W911NF-10-2-0060, and the Rosen Center for Advanced Computing. Any views or conclusions expressed in this document are those of the authors and do not necessarily reflect or represent the views or official policies, expressed or implied, of NSF, NRL, ONR, ARL, or the U.S. Government. The U.S. Government is authorized to reproduce and distribute reprints for Government purposes, notwithstanding any copyright notation herein.

## References

Baillargeon, R. (1986). Representing the existence and the location of hidden objects: Object permanence in 6- and 8-month-old infants. *Cognition*, *23*, 21–41.

Baillargeon, R. (1987). Object permanence in $3\frac{1}{2}$- and $4\frac{1}{2}$-month-old infants. *Developmental Psychology*, *23*, 655–64.

Bajcsy, R. (1988). Active perception. *Proceedings of the IEEE* (pp. 966–1005). IEEE Press.

Bohg, J., Johnson-Roberson, M., León, B., Felip, J., Gratal, X., Bergstrom, N., Kragic, D., & Morales, A. (2011). Mind the gap - robotic grasping under incomplete observation. *Proceedings of the IEEE International Conference on Robotics and Automation* (pp. 686–693). IEEE Press.

Bratman, M. E. (1990). What is intention? In P. R. Cohen, J. Morgan, & M. E. Pollack (Eds.), *Intentions in communication*, 15–32. Cambridge, MA: MIT Press.

Bratman, M. E., Israel, D. J., & Pollack, M. E. (1988). Plans and resource-bounded practical reasoning. *Computational Intelligence*, *4*, 349–355.

Cohen, P. R., & Levesque, H. J. (1990). Intention is choice with commitment. *Artificial Intelligence*, *42*, 213–361.

Dempster, A. P., Laird, N. M., & Rubin, D. B. (1977). Maximum likelihood from incomplete data via the EM algorithm. *Journal of the Royal Statistical Society B*, *39*, 1–38.

Freyd, J. J., Pantzer, T. M., & Cheng, J. L. (1988). Representing statics as forces in equilibrium. *Journal of Experimental Psychology, General*, *117*, 395–407.

Gupta, A., Efros, A., & Hebert, M. (2010). Blocks world revisited: Image understanding using qualitative geometry and mechanics. *Proceedings of the Eleventh European Conference on Computer Vision* (pp. 482–96). Springer.

Hobbs, J., Stickel, M., Appelt, D., & Martin, P. (1993). Interpretation as abduction. *Artificial Intelligence*, *63*, 69–142.

Hoiem, D., Efros, A. A., & Hebert, M. (2011). Recovering occlusion boundaries from an image. *International Journal of Computer Vision*, *91*, 328–46.

Land, A. H., & Doig, A. G. (1960). An automatic method of solving discrete programming problems. *Econometrica*, *28*, 497–520.

Lauriere, J.-L. (1978). A language and a program for stating and solving combinatorial problems. *Artificial Intelligence*, *10*, 29–127.

Lee, D. C., Hebert, M., & Kanade, T. (2009). Geometric reasoning for single image structure recovery. *Proceedings of the 2009 IEEE Conference on Computer Vision and Pattern Recognition*.

Mackworth, A. K. (1977). Consistency in networks of relations. *Artificial Intelligence*, *8*, 99–118.

Maver, J., & Bajcsy, R. (1993). Occlusions as a guide for planning the next view. *IEEE Transactions on Pattern Analysis and Machine Intelligence*, *15*, 417–33.

Moore, R. C. (1982). *The role of logic in knowledge representation and commonsense reasoning* (Technical Report 264). SRI International, Menlo Park, CA.

Mösenlechner, L., & Beetz, M. (2011). Parameterizing actions to have the appropriate effects. *Proceedings of the IEEE/RSJ International Conference on Intelligent Robots and Systems*.

Rao, A. S., & Georgeff, M. P. (1991). Modeling rational agents within a BDI-architecture. *Proceedings of the Second International Conference on Principles of Knowledge Representation and Reasoning* (pp. 473–84). MA: Morgan-Kaufmann.

Saxena, A., Sun, M., & Ng, A. Y. (2007). Learning 3-d scene structure from a single still image. *Proceedings of the ICCV Workshop on 3D Representation for Recognition*. Rio de Janeiro, Brazil.

Saxena, A., Sun, M., & Ng, A. Y. (2008). Make3d: Learning 3d scene structure from a single still image. *IEEE Transactions on Pattern Analysis and Machine Intelligence*, *31*, 824–40.

Siddharth, N., Barbu, A., & Siskind, J. M. (2011). A visual language model for estimating object pose and structure in a generative visual domain. *Proceedings of the IEEE International Conference on Robotics and Automation* (pp. 4854–60). Shanghai, China: IEEE Press.

Streri, A., & Spelke, E. S. (1988). Haptic perception of objects in infancy. *Cognitive Psychology*, *20*, 1–23.

Wynn, K. (1998). Psychological foundations of number: Numerical competence in human infants. *Trends in Cognitive Sciences*, *2*, 296–303.